Impact of updating vegetation information on land surface model performance

Melissa Ruiz-Vásquez[1,2], Sungmin O[3], Gabriele Arduini[4], Souhail Boussetta[4], Alexander Brenning[2], Ana Bastos[1], Sujan Koirala[1], Gianpaolo Balsamo[4], Markus Reichstein[1], and René Orth[1]

[1]Department of Biogeochemical Integration, Max Planck Institute for Biogeochemistry, Jena, Germany
[2]Friedrich Schiller University Jena, Department of Geography, Jena, Germany
[3]Department of Climate and Energy System Engineering, Ewha Womans University, Seoul, South Korea
[4]Research Department, European Centre for Medium-Range Weather Forecasts, Reading, UK

Key Points:

- We find a substantial impact on the ECLand simulated latent heat flux and soil moisture after updating land surface information
- A regional calibration of land surface related parameters yields substantial better agreement between model simulations and observations
- Our results highlight the importance of representing vegetation dynamics and land cover changes in land surface models

Corresponding author: Melissa Ruiz-Vásquez, `mruiz@bgc-jena.mpg.de`

Abstract

Vegetation plays a fundamental role in modulating the exchange of water, energy, and carbon fluxes between the land and the atmosphere. These exchanges are modelled by Land Surface Models (LSMs), which are an essential part of numerical weather prediction and data assimilation. However, most current LSMs implemented specifically in weather forecasting systems use climatological vegetation indices, and land use/land cover datasets in these models are often outdated. In this study, we update land surface data in the ECMWF land surface modelling system ECLand using Earth observation-based time varying leaf area index and land use/land cover data, and evaluate the impact of vegetation dynamics on model performance. The performance of the simulated latent heat flux and soil moisture is then evaluated against global gridded observation-based datasets. Updating the vegetation information does not always yield better model performances because the model's parameters are adapted to the previously employed land surface information. Therefore we recalibrate key soil and vegetation-related parameters at individual grid cells to adjust the model parameterizations to the new land surface information. This substantially improves model performance and demonstrates the benefits of updated vegetation information. Interestingly, we find that a regional parameter calibration outperforms a globally uniform adjustment of parameters, indicating that parameters should sufficiently reflect spatial variability in the land surface. Our results highlight that newly available Earth-observation products of vegetation dynamics and land cover changes can improve land surface model performances, which in turn can contribute to more accurate weather forecasts.

Plain Language Summary

The accuracy of weather forecasts relies critically on the accurate modelling of the exchange of water and energy between the land surface and the atmosphere. The latent heat flux and the soil moisture are two important land surface variables in this exchange through the net balances of water and energy. The accurate simulation of these variables is challenging in most land surface models specifically used for numerical weather prediction due to *i*) outdated land surface cover information and/or *ii*) neglecting the role of short-term anomalies in vegetation functioning, e.g. related to droughts. This study quantifies the benefits of including up-to-date land use/land cover information and an explicit consideration of the current vegetation state on the prediction of latent heat flux and soil moisture. We find that model simulation performance can only benefit from updated land surface information through further adjustments to key soil and vegetation related parameters in the model. Overall, we demonstrate that the new Earth observation datasets can help to improve land surface model performance, which then contributes to more accurate weather forecasts.

1 Introduction

The atmosphere is sensitive to variations in land surface processes, and such covariability between the land and atmosphere states is described as the land-atmosphere coupling (Santanello et al., 2009; Quillet et al., 2010; Santanello et al., 2018). The land surface characteristics, e.g. vegetation state, albedo, and soil moisture, play important roles in this coupling as they modulate the exchange of water, energy, and carbon between the land surface and the atmosphere (Balsamo et al., 2011; de Rosnay et al., 2013; Dirmeyer et al., 2018). Accordingly, an adequate representation of land surface properties in the land surface models that are specifically used in numerical weather prediction (hereafter LSMs) contributes to improved forecast skills from short-range weather forecasts to long-range seasonal predictions (Guo et al., 2011; Dirmeyer & Halder, 2017; Nogueira et al., 2020), helping to better predict extreme events like heat waves or droughts (Zhang et al., 2008; Meng et al., 2014; Hirsch et al., 2019; Miralles et al., 2019).

As LSMs are an essential component of the models that are typically used for weather forecasting systems, there have been considerable efforts in recent decades to improve LSM performance (Wipfler et al., 2011; Dutra et al., 2010; Laguë et al., 2019; Fisher & Koven, 2020). The constantly increasing computing power allows us to include more realistic descriptions of relevant processes and their interactions with the atmosphere, including soil thermodynamics, vegetation dynamics, and land cover and management (Nemunaitis-Berry et al., 2017; González-Rouco et al., 2021; Steinert et al., 2021). Another reason for this improvement is the increasing availability of Earth observation data that allows to characterise surface properties and better constrain model simulations (Ghilain et al., 2012; Orth et al., 2017; Balsamo et al., 2018; Hawkins et al., 2019). For LSMs that employ data assimilation, such as the Carbon Cycle Data Assimilation System (CCDAS) (Rayner et al., 2005) and ORCHIDEE (Santaren et al., 2007), Earth observation constitutes an important data source for key land surface variables including soil moisture, vegetation state, albedo, and land use/land cover (Guillevic et al., 2002; Seneviratne et al., 2010; Meng et al., 2014). However, exploiting these new data streams for enhanced land surface model performance is not straightforward (Wulfmeyer et al., 2018).

Traditional LSMs used for weather forecasting incorporate the effect of vegetation on simulated land surface meteorology through look-up-tables providing different parameter values depending on the biome type (Boussetta et al., 2013; Johannsen et al., 2019; Duveiller et al., 2022). This requires up-to-date information on land cover described through the considered biome types. Furthermore, state-of-the-art LSMs use satellite-observed vegetation indices such as the leaf area index (LAI) to describe vegetation greening, maturity, and senescence (Boussetta et al., 2013; Stevens et al., 2020). However, in most LSMs, the vegetation state is represented only through climatological seasonality, neglecting possible impacts of anomalies in vegetation functioning on the weather (Duveiller et al., 2022). Therefore, the full potential of LSMs in the face of the newly available Earth observation data is not yet well exploited, resulting in opportunities for further improving weather prediction accuracy.

In this study, we use the ECMWF land surface modelling system ECLand based on the previous Hydrology Tiled ECMWF Surface Scheme for Exchange over Land (HTESSEL) to investigate the impact of updating vegetation and land cover information on model performance (Boussetta et al., 2021). Previous studies have found that updating the vegetation information in HTESSEL enhances the performance of simulated soil moisture and energy fluxes thanks to a more accurate representation of *i*) the soil moisture uptake and *ii*) the modulation of evapotranspiration in response to soil moisture changes (Boussetta et al., 2013, 2015; Orth et al., 2017; Nogueira et al., 2020; O et al., 2020; Stevens et al., 2020). More recent studies that use the coupled version of HTESSEL within the Integrated Forecasting System (IFS) show the subsequent effect of updated land surface information on the forecast skill. For instance, Johannsen et al. (2019) showed that large biases in temperature simulated by the IFS strongly relate to the outdated land cover representation within HTESSEL. Further, Nogueira et al. (2021) showed that it is necessary to adapt the model to the new data, i.e., to perform a recalibration of model parameters. This recalibration is an important step in the process of exploiting the potential of updated land surface information since the model is well adapted to the previously used data. However most existing studies overlook the importance of model recalibration, partially due to the lack of land observations to constrain the model parameters (Orth et al., 2016).

Even though there have been considerable efforts to exploit additional Earth observations with HTESSEL, they have never brought together all updates in one single study, nor have they performed this in combination with a parameter recalibration. Building upon the most recent HTESSEL model performance studies, we perform a comprehensive analysis with updated land surface information in ECLand as follows: *i*) we update the land use/land cover information using the ESA-CCI/C3S dataset; *ii*) we introduce interannual variability of LAI and land cover fraction from Sentinel-3 and THEA GEOV2; *iii*) we perform a recalibration of key model parameters to adjust the model parameterizations to the newly updated land cover and vegetation information. This way, we explore the contribution of near-real time land surface information and model calibration to model performance.

2 Data and methods

2.1 List of modelling experiments

We perform multiple uncoupled model experiments while continuously updating the land and vegetation information of ECLand, as listed in Table 1. We use meteorological forcing from ERA5 (Hersbach et al., 2020) at a reduced Gaussian grid of approximately 0.5° spatial resolution and hourly temporal resolution, from 1 January 1995 to 31 December 2019. The temperature, surface pressure, humidity and wind fields are instantaneous values and representative of the atmospheric layer at 10 m above the surface. The incoming shortwave and longwave radiation at the surface, rainfall and snowfall are provided as hourly accumulations (Boussetta et al., 2015). We use a spin-up period from 1995-1999, and all results shown do not include these five years.

Table 1. Modelling experiments with ECLand

Experiment	Land cover dataset	Cover fraction dynamics	LAI dynamics	Land surface parameters
CONTROL	GLCC	Climatology	Climatology	Default
LC	ESA-CCI/C3S	Climatology	Climatology	Default
LC_COV	ESA-CCI/C3S	Interannual variability	Climatology	Default
LC_LAI	ESA-CCI/C3S	Climatology	Interannual variability	Default
LC_COV_LAI	ESA-CCI/C3S	Interannual variability	Interannual variability	Default
Global calibration	ESA-CCI/C3S	Interannual variability	Interannual variability	Spatially constant calibration
Regional calibration	ESA-CCI/C3S	Interannual variability	Interannual variability	Regionally varying calibration

For each experiment, we update one aspect of the land surface model, i.e. land cover, cover fraction, LAI or land surface parameters. We start from a baseline simulation (CONTROL) which is based on an outdated land cover dataset from the USGS Global Land Cover Characterization (GLCC) (Loveland et al., 2000), cover fraction and LAI climatology, and default model parameters, until we perform the LC_COV_LAI experiment in which we update all aspects including the land cover dataset using information from ESA-CCI/C3S (Bontemps et al., 2017), the cover fraction interannual variability and the LAI interannual variability using 10-daily data from Sentinel-3 (Verger et al., 2022) and THEA GEOV2 (Verger et al., 2020), but with default model parameters. The cover fraction and LAI interannual variability refers to monthly values that vary every year, in contrast to climatological monthly means, based on the monthly mean calculated over the period 1993-2019.

We additionally perform two calibration experiments (last two rows in Table 1) in which we recalibrate six soil- and vegetation-related model parameters listed in Table 2: *i*) a global calibration in which we search a unique parameter set that works best overall for all selected grid cells (i.e. spatially constant calibration), and *ii*) a regional calibration in which we define the best parameter set individually for each grid cell (i.e. regionally varying calibration). We use Latin hypercube sampling (McKay et al., 1979) to select 1000 random combinations of perturbation factors independently chosen for each parameter within a specified range. The selection of the range for each parameter follows previously used ranges in recent literature about parameter sensitivity analysis and recalibration of similar parameters in HTESSEL (MacLeod et al., 2016; Orth et al., 2016, 2017; Johannsen et al., 2019; O et al., 2020; Stevens et al., 2020).

Table 2. Model parameters considered for the recalibration experiments

Model parameter	Units	Range of default values	Range of perturbation factors
Hydraulic conductivity	ms^{-1}	0.83–3.83	0.01–100.0
Humidity stress function	$ms^{-1}mbar$	0.00–0.03	0.25–4.0
Minimum stomatal resistance	sm^{-1}	80–250	0.25–4.0
Soil moisture stress function	-	-	0.25–4.0
Total soil depth	cm	1–800	0.5–2.0
Transmission of net solar radiation through vegetation	-	0.03–0.05	0.1–10.0

For computational efficiency, we perform the parameter calibration experiments only at 230 randomly chosen grid cells across the globe (their location is shown in global maps at Section 3.2.2). We only consider grid cells with a long-term mean Enhanced Vegetation Index (EVI) greater than 0.2 to exclude regions with scarce vegetation. The EVI data are derived from MODIS V6 (Didan, 2015). First, we select 30 grid cells to run the 1000 simulations (one for each parameter set), and we select the best 100 parameter sets according to the model performance metric introduced in Section 2.2. Second, we run the best 100 parameter sets in the remaining 200 grid cells and we again evaluate their performance to find the best-performing parameters that work over a wider range of climate regimes.

2.2 Model evaluation

For each model experiment, we compare simulated latent heat flux and soil moisture with respective global gridded observation-based datasets listed in Table 3. While we use absolute values for latent heat flux, for near-surface and deep soil moisture we analyze normalized anomalies to account for different systematic errors in ECLand and in each reference dataset. To compute normalized anomalies for each soil moisture variable and dataset *i*) we subtract the linear long-term trend from the time series, *ii*) we remove the mean seasonal cycle calculated at daily time steps over the period 2000-2019, and *iii*) we divide by the standard deviation of the resulting time series.

Table 3. Reference datasets for model performance evaluation

Output variable	Reference dataset	Source of information
Near-surface soi lmoisture normalized anomalies	SoMo.ml 0-10 cm soil layer (upscaled in situ observations)	O and Orth (2021)
	GLEAM 0-10 cm soil layer (physical-based model)	Martens et al. (2017)
	MERRA-2 0-5 cm soil layer (reanalysis)	Gelaro et al. (2017)
Deep soil moisture normalized anomalies	SoMo.ml 10-50 cm soil layer (upscaled in situ observations)	O and Orth (2021)
	GLEAM 10-100 cm soil layer (physical-based model)	Martens et al. (2017)
	MERRA-2 0-100 cm soil layer (reanalysis)	Gelaro et al. (2017)
Surface latent heat flux	FLUXCOM RS V6 (upscaled in situ observations)	Jung et al. (2019)
	GLEAM (physical-based model)	Martens et al. (2017)
	MERRA-2 (reanalysis)	Gelaro et al. (2017)

We use censored RMSE (cenRMSE) as a performance metric, which is based on modified root mean squared error (RMSE) to account for uncertainties in the observational data. The term “censored” refers to a value that occurs outside the range of a measuring instrument (Fridley & Dixon, 2007). We compute the cenRMSE as follows:

$$cenRMSE = \sqrt{\sum_{i=1}^{n} dy_i^2} \tag{1}$$

$$dy_i = min(|\hat{y}_i - y_{i,r}|), r = 1, 2, 3 \tag{2}$$

$\hat{y}_i$ is the model value in time step i and $y_{i,r}$ is the reference data for the three references ($y_{i,1}$, $y_{i,2}$. $y_{i,3}$). $dy_i = 0$ if $\hat{y}_i$ is in the interval defined by the range of the reference values, otherwise the minimum is taken to compute the cenRMSE. The cenRMSE behaves like RMSE outside the interval and is 0 if all predictions are within the range of reference values.

Specifically for the parameter calibration experiments, we combine the cenRMSE performance metric of the three target variables (i.e. near-surface soil moisture, deep soil moisture and surface latent heat flux). We rank the 1000 perturbation factors individually for each variable and then we add the individual ranks up. The lowest (highest) sums constitute the best (poorest) perturbation factors in terms of model performance.

2.3 Spatial variability of regional parameters

We extend our analysis to the spatial features of calibrated model parameters (Table 2). We employ random forest models (Breiman, 2001; Molnar, 2020) (hereafter RF) to predict each of the six calibrated parameter values across grid pixels (six RF models are used). As predictor variables we use *i*) long-term mean climatic and land surface characteristics such as aridity, temperature and EVI, *ii*) differences in high and low vegetation cover between the two land cover datasets used in the modelling experiments (ESA-CCI/C3S and GLCC) (Boussetta et al., 2021), and *iii*) the values of the remaining five parameters (other than the target parameter). This allows us to determine if there is a spatial pattern of the newly defined model parameters and, if so, to quantify factors influencing the spatial patterns.

We use information from the 230 grid cells for the RF training. We assess the performance of the RF models by computing the R^2 between the predicted and the observed target variables for out-of-bag (OOB) data that was not used for training (hereafter referred to as estimate of R^2) (Li et al., 2021). We infer the relative importance of each predictor variable from SHapley Additive exPlanations (SHAP) feature importance which is based on the average marginal contribution of each predictor to the modelled target variable (Lundberg & Lee, 2017; Sundararajan & Najmi, 2020).

We note a potential caveat in our approach with the RF due to existing relationships among our selected set of predictors. Accordingly, we compute individual Spearman correlations (Wilks, 2011) among the predictors to account for the magnitude of these associations and to identify the most affected variables.

3 Results and discussion

3.1 Impact of updated land surface information on model performance

Figure 1 shows ECLand's model performance in the CONTROL experiment. In general, the model performance varies considerably across regions. For near-surface and deep soil moisture (Figure 1 a and b), we see relatively good performance in the mid-latitudes of Europe, North America and southern South America. On the contrary, the model performs poorly in high-latitude regions, possibly due to high uncertainty in soil moisture-related processes, e.g, soil freeze/thaw cycles (Dutra et al., 2010, 2011; Diro et al., 2018). In some regions, the model performance for deep soil moisture is slightly poorer than for near-surface soil moisture. This can be due to the high uncertainty among the reference datasets for deep soil moisture values as a consequence of sparse observations (Denissen et al., 2020; Koster et al., 2020; Li et al., 2021). For the surface latent heat flux (Figure 1 c) the cenRMSE is relatively good in central and eastern Europe and North America, which might be related to the high density of observations that can support model development and parameter calibration dedicated to these regions (Stegehuis et al., 2013).

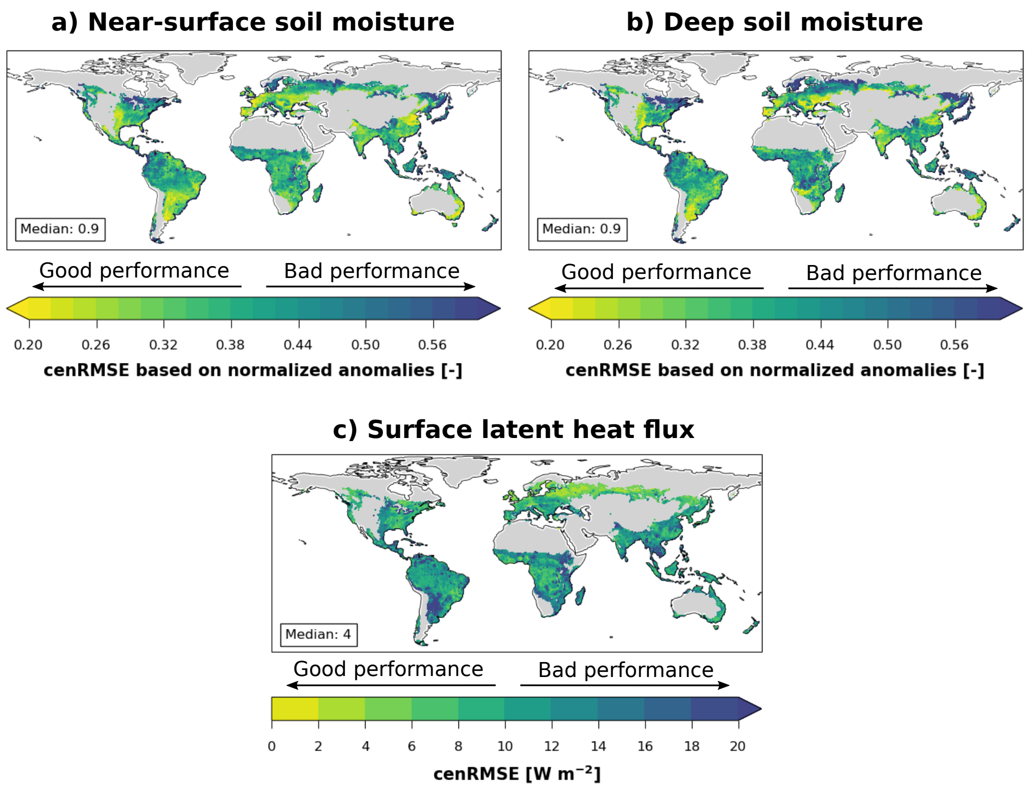

Figure 1. cenRMSE performance metric of CONTROL simulation for a) near-surface soil moisture, b) deep soil moisture and c) surface latent heat flux. cenRMSE is computed based on absolute values for latent heat flux, while normalized anomalies are used for soil moisture. Numbers in the textboxes represent the global median. Gray areas are masked as their long-term mean EVI is lower than 0.2.

Figure 2 shows the performance of the experiment with the most updated land information (LC_COV_LAI) compared to the performance of the CONTROL experiment. We find a general deterioration of model performance (red color) for all three variables considered which is related to the high sensitivity of the RMSE-based metrics to outliers. Recomputing the cenRMSE without the 10% largest disagreements between LC_COV_LAI and CONTROL simulation confirms that the percentage difference in cenRMSE improves in most regions (not shown). Therefore, on average, an update of the land surface information in ECLand has positive impacts on the prediction of surface latent heat flux and near-surface and deep soil moisture.

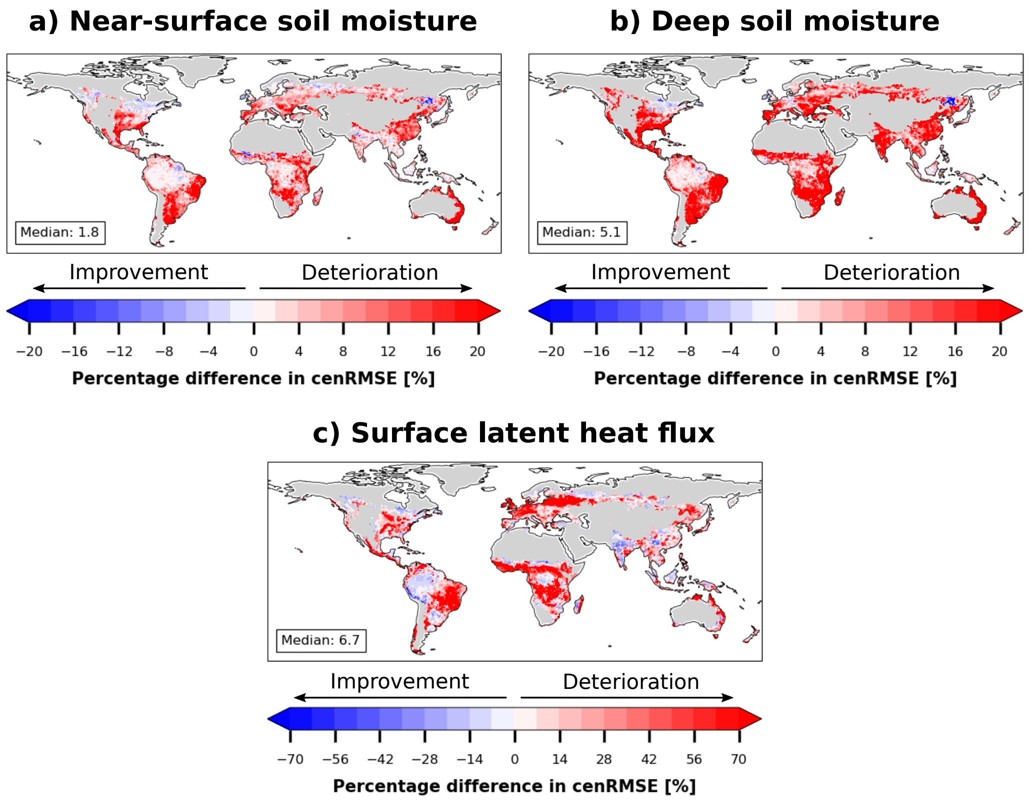

Figure 2. Similar to Figure 1, but for percentage differences in performance: LC_COV_LAI minus CONTROL divided by CONTROL.

The updated land surface information has a much clearer impact on the simulation of latent heat flux compared to soil moisture, as indicated by a larger magnitude of percentage changes in surface latent heat flux. Also, the spatial patterns of improvement/deterioration are not always consistent between latent heat flux and soil moisture; for instance, in southern South America there is improvement in most areas for surface latent heat flux but for both near-surface and deep soil moisture we find deterioration. This points to possible weaknesses in the representation of the coupling between latent heat flux and soil moisture in the model, as also stated in other studies (Zhang et al., 2008; Santanello et al., 2009; Quillet et al., 2010; Meng et al., 2014; Dirmeyer & Halder, 2017; Wulfmeyer et al., 2018; Fairbairn et al., 2019).

We also look at the model performance of each individual experiment in terms of the three considered output variables (Figures S1, S2 and S3). In general, the spatial patterns of improvement and deterioration are similar to the results in Figure 2. Comparing the magnitudes of the changes we find that the strongest effect on the model performance is exerted by the land cover type update, which is present in all experiments. The LAI interannual variability update has the second strongest effect on the model performance (Boussetta et al., 2013, 2015; Stevens et al., 2020; Duveiller et al., 2022).

3.2 Effect of recalibration of model parameters

3.2.1 Ranks of the parameter sets

We rank the 1000 model simulations with perturbed parameter values according to the cenRMSE performance metric of the three target variables (see Section 2.2), and relate the ranking to individual parameter perturbations in Figure 3 in order to assess their individual contribution. Table S1 shows the individual optimal perturbation factors for the model parameters. Hydraulic conductivity and minimum stomatal resistance show the strongest systematic influence on model performance, similar to the results from Orth et al. (2016) and Orth et al. (2017).

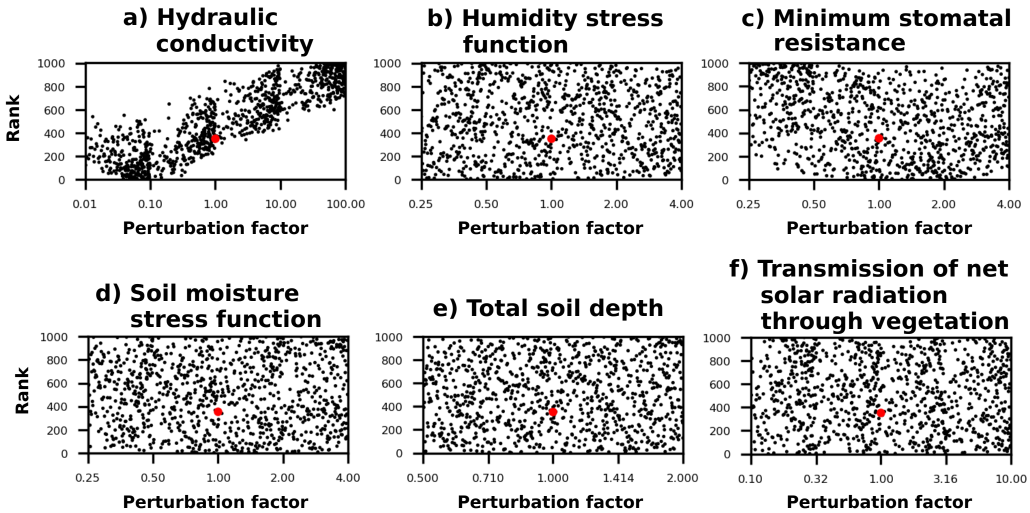

Figure 3. Relating model performance to perturbations in the considered individual ECLand parameters: a) hydraulic conductivity, b) humidity stress function, c) minimum stomatal resistance, d) soil moisture stress function, e) total soil depth and f) transmission of net solar radiation through vegetation. Red dots indicate the performance of the default parameterizations (i.e. no perturbation). A rank value of 1 (1000) in the Y-axis indicates the best (poorest) perturbation factor in model performance.

Hydraulic conductivity governs the water transport in the soil and is therefore directly linked to soil moisture and evapotranspiration (latent heat flux). We find that a substantial reduction of the hydraulic conductivity from its default value improves model performance. This reduces percolation of infiltrated water and therefore increases near-surface soil moisture and ultimately latent heat flux (O et al., 2020). If the model with the new land surface information displays a general dry bias in soil moisture, a lower hydraulic conductivity would help in retaining more water into the soil matrix.

In the case of the minimum stomatal resistance it strongly relates to evapotranspiration as it modulates the exchange of moisture from vegetated surfaces (Orth et al., 2016). Our results suggest that there is an optimum perturbation value for the minimum stomatal resistance between 1 and 2, i.e. close to the default parameterization, thus, modifying it has little potential to improve the model. The increase in stomata resistance should be related to an excess of evapotranspiration with the new land surface information, for instance, with an increase of LAI, compared to the CONTROL experiment.

We also analyze the influence of parameter perturbations on model performance in terms of the considered individual variables (Figures S4, S5 and S6). The clear pattern of better model performance in the case of lower hydraulic conductivity found in Figure 3 is mainly related to an improvement of the soil moisture performance, especially for the near-surface layer (Figure S4). For the minimum stomatal resistance the pattern found in Figure 3 is related to variations in the simulation performance of latent heat flux (Figure S6). Additionally, the total soil depth is relevant for the simulation performance of deep soil moisture, (Figure S5) as also found in a similar study by Hawkins et al. (2019). This illustrates that different parameters matter for different land surface variables, as well as that different observational datasets are needed to constrain different parameters.

3.2.2 Model performance in parameter calibration experiments

Figures 4 and 5 show the model performance changes relative to CONTROL after the global and the regional recalibration across 230 grid cells, respectively. Generally, for the global calibration (Figure 4) we find inconsistent results with improved or deteriorated model performance depending on the grid cell. This suggests that there is no one(calibration)-fits-all(regions) solution, probably related to the spatial heterogeneity in climate along with different land surface characteristics, or its insufficient representation in the current default values in the model (like for specific vegetation types, soil textures, etc.) (Laguë et al., 2019; Nogueira et al., 2021), as can be seen from the spatial distribution of the calibrated parameter values in Figure S7. After the global calibration we already see an improvement in both soil moisture variables but it is not always the case for the surface latent heat flux, probably due to compensation in model performance between variables (McCabe et al., 2005). This is expected as the newly applied datastreams are related to land cover and vegetation structure. Specifically, the model performance in the grid cells in northern Asia always degrades from a global calibration, whereas for the other regions we see mixed results.

After the regional calibration, we find substantial improvement in model performance for all three variables as shown in Figure 5. See also Figure S8 for comparisons of model performance between the regional and global calibrations. In a similar study for another LSM, Xie et al. (2007) found an improvement in model performance after a regional calibration of model parameters. This suggests that parameters should sufficiently reflect land surface heterogeneity, different climate zones, different biome types, etc. The regional calibration leads to better model performance for most grid pixels, except for high latitudes in Northern Asia, possibly due to high uncertainty in the representation of soil freeze processes, as found in other studies (Dutra et al., 2010, 2011; Diro et al., 2018).

To aggregate our main findings, Figure 6 shows the median global change in model performance for each experiment and variable. Most of the experiments do not show clear model performance improvement with regards to the CONTROL simulation before recalibration. Only the regional calibration experiment shows improvement in all output variables, which calls for parameter recalibration after updating land surface information on LSMs to exploit the benefits of Earth observation developments (Nogueira et al., 2021). This is specifically the case for a regional (spatially varying) as opposed to the global (spatially constant) calibration as this can better account for spatial heterogeneities, and compensate for potentially related shortcomings in the model structure (Xie et al., 2007). The variability of the experiments (represented by the error bars in Figure 6) for the surface latent heat flux is higher than for the two soil moisture variables. We attribute this to a direct effect on latent heat flux from the perturbation of the selected parameters because these are mostly related with evapotranspiration, whereas they have an indirect effect on soil moisture (Jefferson et al., 2017; Montzka et al., 2017).

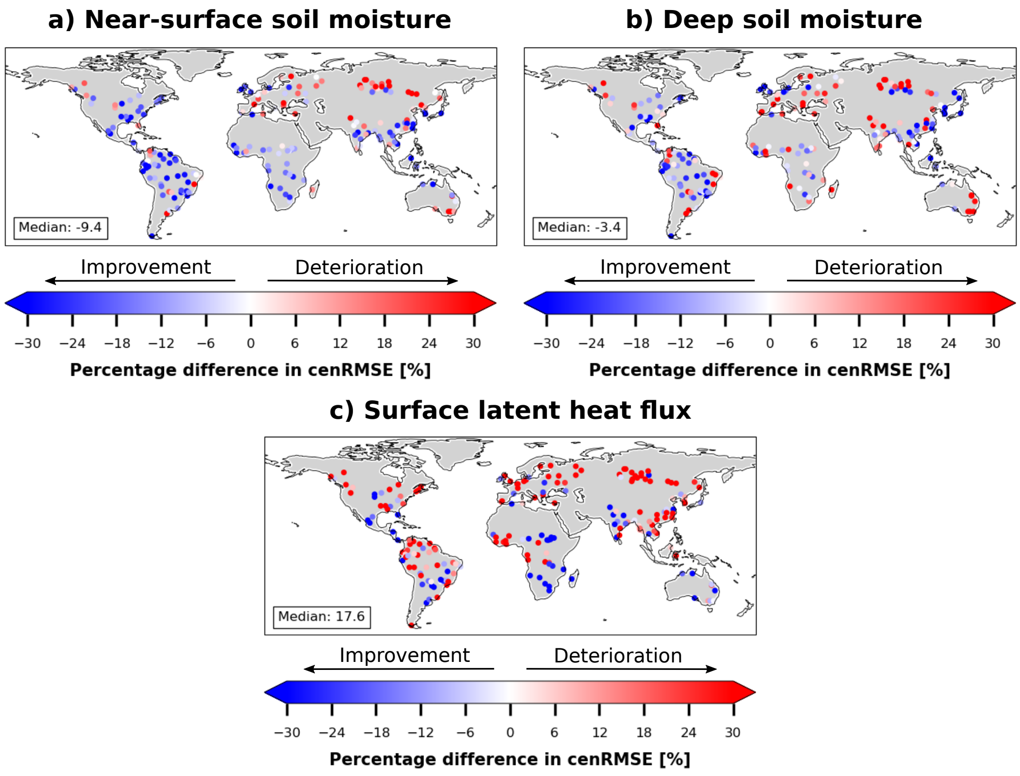

Figure 4. Similar to Figure 1, but for percentage differences in performance: Global calibration minus CONTROL divided by CONTROL.

In a final step, we study model performance changes in wet vs. dry regions by producing Figure 6 for such regions separately (Figure S9). The effect of updating land surface information in ECLand on model performance is generally stronger in dry grid cells than in wet grid cells. This is expected since vegetation plays a more important role for modulating the exchange of water and energy in dry-to-transitional regions, whereas the role of the vegetation and relevant land processes in comparison to the effect of atmospheric dynamics is less prominent in wet regions (Seneviratne et al., 2010; Miralles et al., 2019; Denissen et al., 2020).

3.3 Attribution analysis of spatial patterns of regional parameter calibration

In a final step, we analyze the spatial patterns of the optimal parameter perturbations determined in the grid cell-wise model calibration shown in Figure S7. In order to explain the spatial pattern of each parameter we consider several predictors including climate and vegetation characteristics, as well as the calibrated values of the other considered parameters. This attribution analysis is done separately for each parameter (target in the regional calibration). Figure 7 shows that overall we see that for each of the modelled parameters, the remaining parameters are the best factors to predict the values of the target. Only for the humidity stress function (Figure 7 b) and for the transmission of net solar radiation through vegetation (Figure 7 f) the difference in vegetation type and the temperature are important predictors (other than the remaining model parameters) in the RF models, respectively. We attribute this to an equifinality problem in the model and accept it as a caveat in our analysis: we select only the best pa-

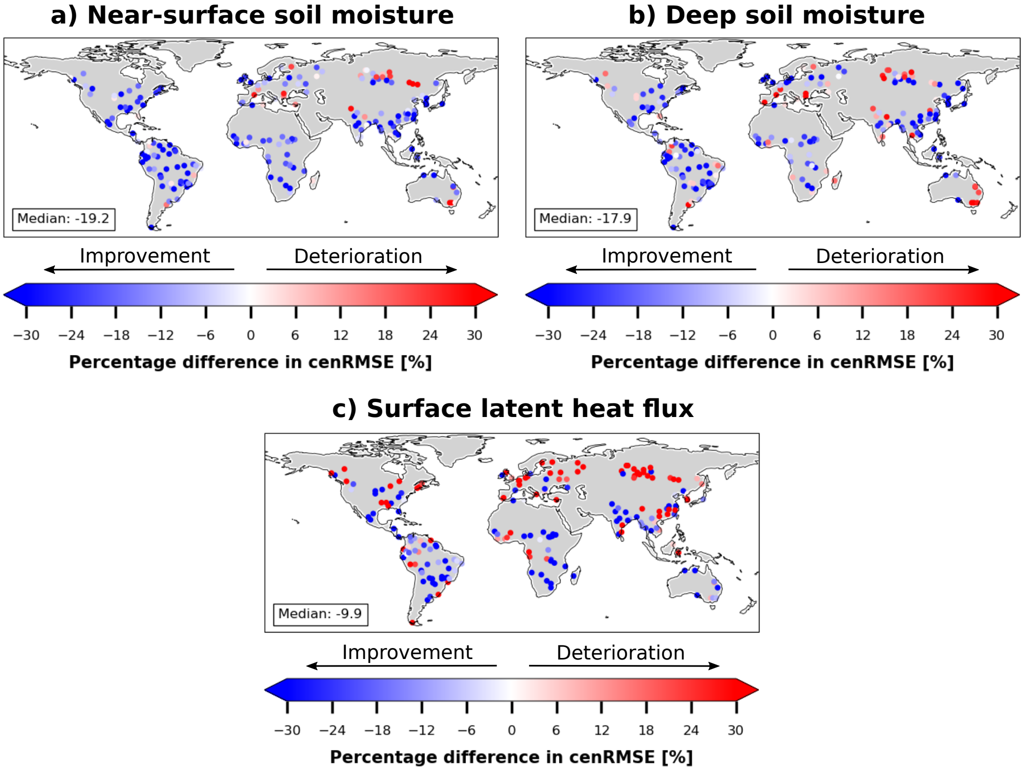

Figure 5. Similar to Figure 1, but for percentage differences in performance: Regional calibration minus CONTROL divided by CONTROL.

rameter sets while other sets might perform almost as good as the best set (Williams et al., 2009).

The RF models have in general a good model performance (Figure S10), meaning that the considered factors can explain the spatial patterns of model parameters. The hydraulic conductivity calibration has the best RF model performance due to the clear systematic pattern in the parameter set ranks (Figure 3 a), specially given by the dependence of the near-surface soil moisture model performance on this parameter (Figure S4).

The relative importance is analyzed here for correlation and not causation. We acknowledge that some of the selected factors are highly correlated (Figure S11) and their actual relative importance might be reduced by the collinearities (Ghosh & Maiti, 2021). The most cross-correlated ones are: hydraulic conductivity and total soil depth; minimum stomatal resistance and soil moisture stress function; EVI and aridity; EVI and temperature; and the differences in high and low vegetation cover. However, most pairs of factors show correlation lower than 0.2.

4 Summary and conclusion

Recent studies performed substantial efforts for exploiting additional Earth observations in ECLand model validation (Boussetta et al., 2013, 2015; Orth et al., 2017; Nogueira et al., 2020; O et al., 2020; Stevens et al., 2020). However these experiments have never

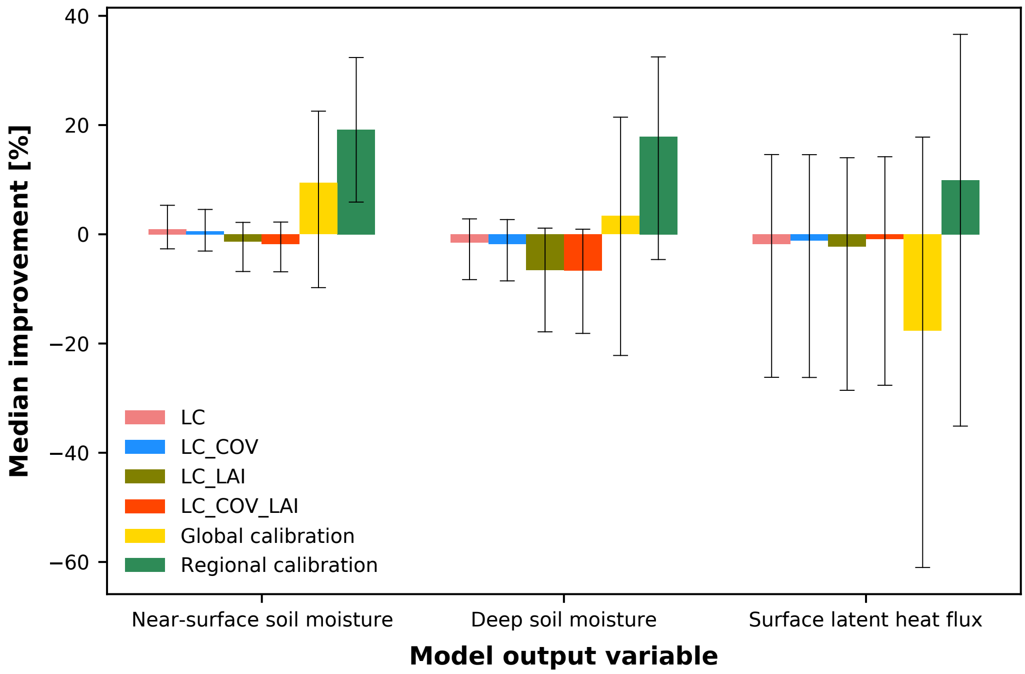

Figure 6. Summary of ECLand performance for each experiment compared to the CONTROL simulation. Medians of percentage change of cenRMSE across 230 grid cells are shown. The error bars represent the 25th and 75th percentile.

included all updates in one single study. Neither have they performed a follow-up recalibration of the model to exploit the benefits of including more accurate land surface information. Here we make a step in this direction with our comprehensive modelling experiments (Gupta et al., 1999), not only updating land cover type but also including interannual variability of LAI and cover fraction.

We find a substantial impact of updating land and vegetation information from newly available Earth observations on the simulated surface latent heat flux and near-surface and deep soil moisture. However, these modifications do not always show positive impacts on the model performance. The changes in model performance vary between regions and considered variables, indicating the need for model evaluation based on multivariable analysis to make conclusive remarks on model performance (McCabe et al., 2005). Further, this shows that ingesting novel Earth observation data streams into current LSMs is not automatically leading to improved model performance as the model parameterizations need to be adapted to these updates (Nogueira et al., 2021). By considering several reference datasets, we benefit from the growing suite of global observational products, and manage to incorporate the uncertainty between these products into our evaluation of model performance.

As a further step we also recalibrate the model to adapt it to the new conditions. For the model recalibration we follow two approaches: global calibration and regional calibration (Xie et al., 2007). We find that the regional calibration yields substantial better agreement between model simulations and reference datasets, suggesting it may be beneficial to revise the spatial variability of model parameters which so far is based on soil and vegetation types (i.e. look-up tables). An update of those look-up tables and/or

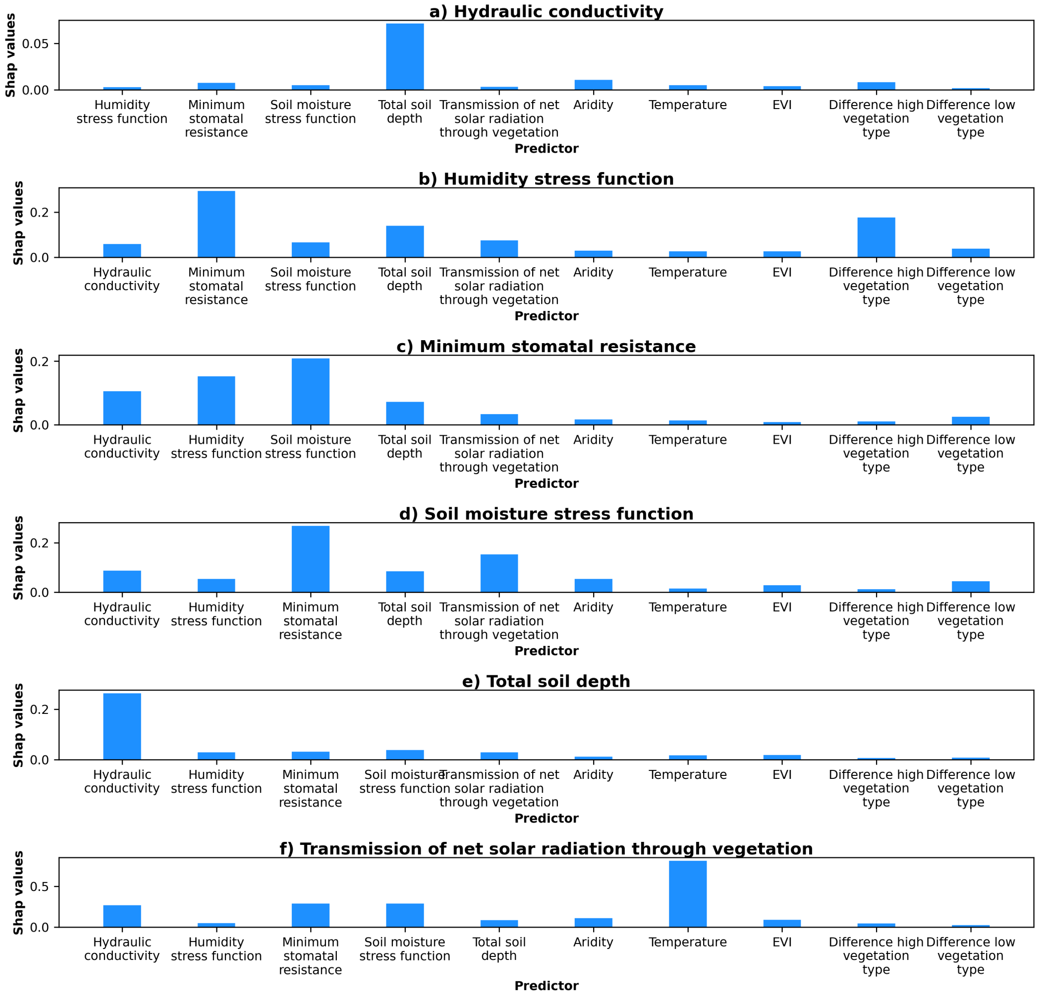

Figure 7. Relative importance (SHAP values) of multiple factors to explain the spatial patterns of regionally calibrated model parameters for a) hydraulic conductivity, b) humidity stress function, c) Minimum stomatal resistance, d) soil moisture stress function, e) total soil depth and f) transmission of net solar radiation through vegetation. Note that the Y-axes have different ranges.

the consideration of more aspects of spatial heterogeneity may be a way forward in this context. This would allow that future calibrations can be done globally only.

We suggest that one reason for the lack of improvement in the model performance after updating land surface information with state-of-the-art observations is attributed to the then outdated model parameters. The model shows substantial improvement when adjusting parameters, particularly through the regional calibration, indicating that land information updates in the model cannot be treated independently from model parameterization. Future work should consider the impact of the improved and calibrated ECLand performance within a coupled model system.

Open Research Section

The meteorological forcing for ECLand from ERA5 is available at https://cds.climate.copernicus.eu/ (ECMWF & Service, 2018). The EVI data from MODIS are available through NASA's data catalogue at https://lpdaac.usgs.gov/products/mod13c1v006/ (EOSDIS, 2015). Both the evaporative fraction data from FLUXCOM and the soil moisture data from SoMo.ml are available at the Data Portal of the Max Planck Institute for Biogeochemistry at https://www.bgc-jena.mpg.de/geodb/projects/Data.php (for Biogeochemistry, 2019, 2021). The output data from the ECLand modelling experiments are available in the Zenodo repository at `https://doi.org/10.5281/zenodo.7823893`.

Acknowledgments

The authors thank Ulrich Weber for help with retrieving and processing the data, and the Hydrology-Biosphere-Climate Interactions group at the Max Planck Institute for Biogeochemistry for fruitful discussions. Melissa Ruiz-Vásquez acknowledges support from the International Max Planck Research School on Global Biogeochemical Cycles. René Orth is supported by funding from the German Research Foundation (Emmy Noether grant no. 391059971), Sungmin O is supported by funding from the Brain Pool program, provided by the Ministry of Science and ICT through the National Research Foundation of Korea (grant no. NRF-2021H1D3A2A02040136).

References

Balsamo, G., Agusti-Panareda, A., Albergel, C., Arduini, G., Beljaars, A., Bidlot, J., ... Zeng, X. (2018). Satellite and In Situ observations for advancing global Earth surface modelling: A review. *Remote Sensing*, *10*(12). doi: 10.3390/rs10122038

Balsamo, G., Pappenberger, F., Dutra, E., Viterbo, P., & van den Hurk, B. (2011). A revised land hydrology in the ECMWF model: a step towards daily water flux prediction in a fully-closed water cycle. *Hydrological Processes*, *25*(7), 1046-1054. doi: 10.1002/hyp.7808

Bontemps, S., Radoux, J., de Maet, T., Lamarche, C., Moreau, I., Vittek, M., & Defourny, P. (2017). *Land cover CCI algorithm theoretical basis document part III: Classification year 2-1.2* (Tech. Rep. No. 1.2). ESA Climate Change Initiative. Retrieved from `https://www.esa-landcover-cci.org/?q=webfm_send/139`

Boussetta, S., Balsamo, G., Arduini, G., Dutra, E., McNorton, J., Choulga, M., ... Zsoter, E. (2021). ECLand: The ECMWF land surface modelling system. *Atmosphere*, *12*(6). doi: 10.3390/atmos12060723

Boussetta, S., Balsamo, G., Beljaars, A., Kral, T., & Jarlan, L. (2013). Impact of a satellite-derived leaf area index monthly climatology in a global numerical weather prediction model. *International Journal of Remote Sensing*, *34*(9-10), 3520-3542. doi: 10.1080/01431161.2012.716543

Boussetta, S., Balsamo, G., Dutra, E., Beljaars, A., & Albergel, C. (2015). Assimilation of surface albedo and vegetation states from satellite observations and their impact on numerical weather prediction. *Remote Sensing of Environment*, *163*, 111-126. doi: 10.1016/j.rse.2015.03.009

Breiman, L. (2001). Random forests. *Machine Learning*, *45*(1), 5-32. doi: 10.1023/A:1010933404324

Denissen, J. M., Teuling, A. J., Reichstein, M., & Orth, R. (2020). Critical soil moisture derived from satellite observations over Europe. *Journal of Geophysical Research: Atmospheres*, *125*(6), e2019JD031672. doi: 10.1029/2019JD031672

de Rosnay, P., Drusch, M., Vasiljevic, D., Balsamo, G., Albergel, C., & Isaksen, L. (2013). A simplified extended Kalman filter for the global operational soil moisture analysis at ECMWF. *Quarterly Journal of the Royal Meteorological*

Society, *139*(674), 1199-1213. doi: 10.1002/qj.2023

Didan, K. (2015). *MOD13Q1 MODIS/Terra vegetation indices 16-day L3 global 250m SIN grid v006.* NASA EOSDIS Land Processes DAAC. (Accessed: 28 April 2020) doi: 10.5067/MODIS/MOD13Q1.006

Dirmeyer, P. A., & Halder, S. (2017). Application of the Land–Atmosphere coupling paradigm to the operational Coupled Forecast System, version 2 (CFSv2). *Journal of Hydrometeorology*, *18*(1), 85 - 108. doi: 10.1175/JHM-D-16-0064.1

Dirmeyer, P. A., Halder, S., & Bombardi, R. (2018). On the harvest of predictability from land states in a global forecast model. *Journal of Geophysical Research: Atmospheres*, *123*(23), 13,111-13,127. doi: 10.1029/2018JD029103

Diro, G. T., Sushama, L., & Huziy, O. (2018). Snow-Atmosphere coupling and its impact on temperature variability and extremes over North America. *Climate Dynamics*, *50*(7), 2993-3007. doi: 10.1007/s00382-017-3788-5

Dutra, E., Balsamo, G., Viterbo, P., Miranda, P. M. A., Beljaars, A., Schär, C., & Elder, K. (2010). An improved snow scheme for the ECMWF land surface model: Description and offline validation. *Journal of Hydrometeorology*, *11*(4), 899 - 916. doi: 10.1175/2010JHM1249.1

Dutra, E., Kotlarski, S., Viterbo, P., Balsamo, G., Miranda, P. M. A., Schär, C., ... Jonas, T. (2011). Snow cover sensitivity to horizontal resolution, parameterizations, and atmospheric forcing in a land surface model. *Journal of Geophysical Research: Atmospheres*, *116*(D21). doi: 10.1029/2011JD016061

Duveiller, G., Pickering, M., Muñoz Sabater, J., Caporaso, L., Boussetta, S., Balsamo, G., & Cescatti, A. (2022). Getting the leaves right matters for estimating temperature extremes. *Geoscientific Model Development Discussions*, *2022*, 1–26. doi: 10.5194/gmd-2022-216

ECMWF, & Service, C. C. C. (2018). *ERA5 hourly data on single levels from 1959 to present.* Retrieved from `https://cds.climate.copernicus.eu/` (Accessed: 2 January 2023)

EOSDIS, N. (2015). *Nasa eosdis land processes daac: Mod13c1 modis/terra vegetation indices 16-day l3 global 0.05deg cmg v006.* Retrieved from `https://lpdaac.usgs.gov/products/mod13c1v006/` (Accessed: 28 April 2020)

Fairbairn, D., de Rosnay, P., & Browne, P. A. (2019). The new stand-alone surface analysis at ecmwf: Implications for land–atmosphere da coupling. *Journal of Hydrometeorology*, *20*(10), 2023 - 2042. doi: 10.1175/JHM-D-19-0074.1

Fisher, R. A., & Koven, C. D. (2020). Perspectives on the future of land surface models and the challenges of representing complex terrestrial systems. *Journal of Advances in Modeling Earth Systems*, *12*(4), e2018MS001453. doi: 10.1029/2018MS001453

for Biogeochemistry, M. P. I. (2019). *Fluxcom [data set].* Retrieved from `https://www.bgc-jena.mpg.de/geodb/projects/Data.php` (Accessed: 6 January 2022)

for Biogeochemistry, M. P. I. (2021). *Somo.ml [data set].* Retrieved from `https://www.bgc-jena.mpg.de/geodb/projects/Data.php` (Accessed: 6 January 2022)

Fridley, B. L., & Dixon, P. (2007). Data augmentation for a Bayesian spatial model involving censored observations. *Environmetrics*, *18*(2), 107-123. doi: 10.1002/env.806

Gelaro, R., McCarty, W., Suárez, M. J., Todling, R., Molod, A., Takacs, L., ... Zhao, B. (2017). The Modern-Era Retrospective Analysis for Research and Applications, version 2 (MERRA-2). *Journal of Climate*, *30*(14), 5419 - 5454. doi: 10.1175/JCLI-D-16-0758.1

Ghilain, N., Arboleda, A., Sepulcre-Cantò, G., Batelaan, O., Ardö, J., & Gellens-Meulenberghs, F. (2012). Improving evapotranspiration in a land surface model using biophysical variables derived from MSG/SEVIRI satellite. *Hydrology and Earth System Sciences*, *16*(8), 2567–2583. doi: 10.5194/hess-16-2567-2012

Ghosh, A., & Maiti, R. (2021). Soil erosion susceptibility assessment using logistic regression, decision tree and random forest: study on the Mayurakshi river basin of eastern India. *Environmental Earth Sciences*, *80*(8). doi: 10.1007/s12665-021-09631-5

González-Rouco, J. F., Steinert, N. J., García-Bustamante, E., Hagemann, S., de Vrese, P., Jungclaus, J. H., … Navarro, J. (2021). Increasing the depth of a land surface model. part I: Impacts on the subsurface thermal regime and energy storage. *Journal of Hydrometeorology*, *22*(12), 3211 - 3230. doi: 10.1175/JHM-D-21-0024.1

Guillevic, P., Koster, R. D., Suarez, M. J., Bounoua, L., Collatz, G. J., Los, S. O., & Mahanama, S. P. P. (2002). Influence of the interannual variability of vegetation on the surface energy balance—a global sensitivity study. *Journal of Hydrometeorology*, *3*(6), 617 - 629. doi: 10.1175/1525-7541(2002)003⟨0617:IOTIVO⟩2.0.CO;2

Guo, Z., Dirmeyer, P. A., & DelSole, T. (2011). Land surface impacts on subseasonal and seasonal predictability. *Geophysical Research Letters*, *38*(24). doi: 10.1029/2011GL049945

Gupta, H. V., Bastidas, L. A., Sorooshian, S., Shuttleworth, W. J., & Yang, Z. L. (1999). Parameter estimation of a land surface scheme using multicriteria methods. *Journal of Geophysical Research: Atmospheres*, *104*(D16), 19491-19503. doi: 10.1029/1999JD900154

Hawkins, L. R., Rupp, D. E., McNeall, D. J., Li, S., Betts, R. A., Mote, P. W., … Wallom, D. C. H. (2019). Parametric sensitivity of vegetation dynamics in the TRIFFID model and the associated uncertainty in projected climate change impacts on Western U.S. forests. *Journal of Advances in Modeling Earth Systems*, *11*(8), 2787-2813. doi: 10.1029/2018MS001577

Hersbach, H., Bell, B., Berrisford, P., Hirahara, S., Horányi, A., Muñoz-Sabater, J., … Thépaut, J.-N. (2020). The ERA5 global reanalysis. *Quarterly Journal of the Royal Meteorological Society*, *146*(730), 1999-2049. doi: 10.1002/qj.3803

Hirsch, A. L., Evans, J. P., Di Virgilio, G., Perkins-Kirkpatrick, S. E., Argüeso, D., Pitman, A. J., … Rockel, B. (2019). Amplification of Australian heatwaves via local Land-Atmosphere coupling. *Journal of Geophysical Research: Atmospheres*, *124*(24), 13625-13647. doi: 10.1029/2019JD030665

Jefferson, J. L., Maxwell, R. M., & Constantine, P. G. (2017). Exploring the sensitivity of photosynthesis and stomatal resistance parameters in a land surface model. *Journal of Hydrometeorology*, *18*(3), 897 - 915. doi: 10.1175/JHM-D-16-0053.1

Johannsen, F., Ermida, S., Martins, J. P. A., Trigo, I. F., Nogueira, M., & Dutra, E. (2019). Cold bias of ERA5 summertime daily maximum land surface temperature over Iberian peninsula. *Remote Sensing*, *11*(21). doi: 10.3390/rs11212570

Jung, M., Koirala, S., Weber, U., Ichii, K., Gans, F., Camps-Valls, G., … Reichstein, M. (2019). The FLUXCOM ensemble of global Land-Atmosphere energy fluxes. *Scientific Data*, *6*. doi: 10.1038/s41597-019-0076-8

Koster, R. D., Schubert, S. D., DeAngelis, A. M., Molod, A. M., & Mahanama, S. P. (2020). Using a simple water balance framework to quantify the impact of soil moisture initialization on subseasonal evapotranspiration and air temperature forecasts. *Journal of Hydrometeorology*, *21*(8), 1705 - 1722. doi: 10.1175/JHM-D-20-0007.1

Laguë, M. M., Bonan, G. B., & Swann, A. L. S. (2019). Separating the impact of individual land surface properties on the terrestrial surface energy budget in both the coupled and uncoupled Land–Atmosphere System. *Journal of Climate*, *32*(18), 5725 - 5744. doi: 10.1175/JCLI-D-18-0812.1

Li, W., Migliavacca, M., Forkel, M., Walther, S., Reichstein, M., & Orth, R. (2021). Revisiting global vegetation controls using multi-layer soil moisture. *Geophysical Research Letters*, *48*(11), e2021GL092856. doi: 10.1029/2021GL092856

Loveland, T. R., Reed, B. C., Brown, J. F., Ohlen, D. O., Zhu, Z., Yang, L., & Merchant, J. W. (2000). Development of a global land cover characteristics database and IGBP DISCover from 1 km AVHRR data. *International Journal of Remote Sensing*, *21*(6-7), 1303-1330. doi: 10.1080/014311600210191

Lundberg, S., & Lee, S.-I. (2017). *A unified approach to interpreting model predictions.*

MacLeod, D. A., Cloke, H. L., Pappenberger, F., & Weisheimer, A. (2016). Improved seasonal prediction of the hot summer of 2003 over Europe through better representation of uncertainty in the land surface. *Quarterly Journal of the Royal Meteorological Society*, *142*(694), 79-90. doi: 10.1002/qj.2631

Martens, B., Miralles, D. G., Lievens, H., van der Schalie, R., de Jeu, R. A. M., Fernández-Prieto, D., ... Verhoest, N. E. C. (2017). GLEAM v3: satellite-based land evaporation and root-zone soil moisture. *Geoscientific Model Development*, *10*(5), 1903–1925. doi: 10.5194/gmd-10-1903-2017

McCabe, M., Franks, S., & Kalma, J. (2005). Calibration of a land surface model using multiple data sets. *Journal of Hydrology*, *302*(1), 209-222. doi: 10.1016/j.jhydrol.2004.07.002

McKay, M. D., Beckman, R. J., & Conover, W. J. (1979). A comparison of three methods for selecting values of input variables in the analysis of output from a computer code. *Technometrics*, *21*(2), 239–245. doi: 10.2307/1268522

Meng, X. H., Evans, J. P., & McCabe, M. F. (2014). The impact of observed vegetation changes on Land–Atmosphere feedbacks during drought. *Journal of Hydrometeorology*, *15*(2), 759 - 776. doi: 10.1175/JHM-D-13-0130.1

Miralles, D. G., Gentine, P., Seneviratne, S. I., & Teuling, A. J. (2019). Land-Atmospheric feedbacks during droughts and heatwaves: state of the science and current challenges. *Annals of the New York Academy of Sciences*, *1436*(1), 19 - 35. doi: 10.1111/nyas.13912

Molnar, C. (2020). *Interpretable machine learning.* Lulu. com. Retrieved from `https://christophm.github.io/interpretable-ml-book/`

Montzka, C., Herbst, M., Weihermüller, L., Verhoef, A., & Vereecken, H. (2017). A global data set of soil hydraulic properties and sub-grid variability of soil water retention and hydraulic conductivity curves. *Earth System Science Data*, *9*(2), 529–543. doi: 10.5194/essd-9-529-2017

Nemunaitis-Berry, K. L., Klein, P. M., Basara, J. B., & Fedorovich, E. (2017). Sensitivity of predictions of the urban surface energy balance and heat island to variations of urban canopy parameters in simulations with the WRF model. *Journal of Applied Meteorology and Climatology*, *56*(3), 573 - 595. doi: 10.1175/JAMC-D-16-0157.1

Nogueira, M., Albergel, C., Boussetta, S., Johannsen, F., Trigo, I. F., Ermida, S. L., ... Dutra, E. (2020). Role of vegetation in representing land surface temperature in the CHTESSEL (CY45R1) and SURFEX-ISBA (v8.1) land surface models: a case study over Iberia. *Geoscientific Model Development*, *13*(9), 3975–3993. doi: 10.5194/gmd-13-3975-2020

Nogueira, M., Boussetta, S., Balsamo, G., Albergel, C., Trigo, I. F., Johannsen, F., ... Dutra, E. (2021). Upgrading land-cover and vegetation seasonality in the ECMWF coupled system: Verification with FLUXNET sites, METEOSAT satellite land surface temperatures, and ERA5 atmospheric reanalysis. *Journal of Geophysical Research: Atmospheres*, *126*(15), e2020JD034163. doi: 10.1029/2020JD034163

O, S., Dutra, E., & Orth, R. (2020). Robustness of process-based versus data-driven modeling in changing climatic conditions. *Journal of Hydrometeorology*, *21*(9), 1929 - 1944. doi: 10.1175/JHM-D-20-0072.1

O, S., & Orth, R. (2021). Global soil moisture data derived through machine learning trained with *in-situ* measurements. *Scientific Data*, *8*. doi: 10.1038/s41597-021-00964-1

Orth, R., Dutra, E., & Pappenberger, F. (2016). Improving weather predictability by including land surface model parameter uncertainty. *Monthly Weather Review*, *144*(4), 1551 - 1569. doi: 10.1175/MWR-D-15-0283.1

Orth, R., Dutra, E., Trigo, I. F., & Balsamo, G. (2017). Advancing land surface model development with satellite-based Earth observations. *Hydrology and Earth System Sciences*, *21*(5), 2483–2495. doi: 10.5194/hess-21-2483-2017

Quillet, A., Peng, C., & Garneau, M. (2010). Toward dynamic global vegetation models for simulating vegetation–climate interactions and feedbacks: recent developments, limitations, and future challenges. *Environmental Reviews*, *18*(NA), 333-353. doi: 10.1139/A10-016

Rayner, P. J., Scholze, M., Knorr, W., Kaminski, T., Giering, R., & Widmann, H. (2005). Two decades of terrestrial carbon fluxes from a carbon cycle data assimilation system (CCDAS). *Global Biogeochemical Cycles*, *19*(2). doi: 10.1029/2004GB002254

Santanello, J. A., Dirmeyer, P. A., Ferguson, C. R., Findell, K. L., Tawfik, A. B., Berg, A., . . . Wulfmeyer, V. (2018). Land–Atmosphere interactions: The LoCo perspective. *Bulletin of the American Meteorological Society*, *99*(6), 1253 - 1272. doi: 10.1175/BAMS-D-17-0001.1

Santanello, J. A., Peters-Lidard, C. D., Kumar, S. V., Alonge, C., & Tao, W.-K. (2009). A modeling and observational framework for diagnosing local Land–Atmosphere coupling on diurnal time scales. *Journal of Hydrometeorology*, *10*(3), 577 - 599. doi: 10.1175/2009JHM1066.1

Santaren, D., Peylin, P., Viovy, N., & Ciais, P. (2007). Optimizing a process-based ecosystem model with eddy-covariance flux measurements: A pine forest in southern France. *Global Biogeochemical Cycles*, *21*(2). doi: 10.1029/2006GB002834

Seneviratne, S. I., Corti, T., Davin, E. L., Hirschi, M., Jaeger, E. B., Lehner, I., . . . Teuling, A. J. (2010). Investigating soil moisture–climate interactions in a changing climate: A review. *Earth-Science Reviews*, *99*(3), 125-161. doi: 10.1016/j.earscirev.2010.02.004

Stegehuis, A. I., Teuling, A. J., Ciais, P., Vautard, R., & Jung, M. (2013). Future European temperature change uncertainties reduced by using land heat flux observations. *Geophysical Research Letters*, *40*(10), 2242-2245. doi: 10.1002/grl.50404

Steinert, N. J., González-Rouco, J. F., de Vrese, P., García-Bustamante, E., Hagemann, S., Melo-Aguilar, C., . . . Lorenz, S. J. (2021). Increasing the depth of a land surface model. part II: Temperature sensitivity to improved subsurface thermodynamics and associated permafrost response. *Journal of Hydrometeorology*, *22*(12), 3231 - 3254. doi: 10.1175/JHM-D-21-0023.1

Stevens, D., Miranda, P. M. A., Orth, R., Boussetta, S., Balsamo, G., & Dutra, E. (2020). Sensitivity of surface fluxes in the ECMWF land surface model to the remotely sensed leaf area index and root distribution: Evaluation with tower flux data. *Atmosphere*, *11*(12). doi: 10.3390/atmos11121362

Sundararajan, M., & Najmi, A. (2020). *The many Shapley values for model explanation.*

Verger, A., Descals, A., Lacaze, R., & Cherlet, M. (2022). *Copernicus global land operations "vegetation and energy"* (Tech. Rep. No. l1.10). Copernicus. Retrieved from `https://land.copernicus.eu/global/sites/cgls.vito.be/files/products/CGLOPS1_ATBD_LAI300m-V1.1_I1.10.pdf`

Verger, A., Weiss, M., Baret, F., Pacholczyk, P., & Leroy, M. (2020). *Algorithm theoretical basis document* (Tech. Rep. No. l2.50). Théia and CREAF. Retrieved from `https://www.theia-land.fr/wp-content/uploads/2022/03/`

THEIA-SP-44-0207-CREAF_I2.50-1.pdf
Wilks, D. (2011). Chapter 3 - Empirical distributions and exploratory data analysis. In D. S. Wilks (Ed.), *Statistical methods in the atmospheric sciences* (Vol. 100, p. 23-70). Academic Press. doi: 10.1016/B978-0-12-385022-5.00003-8
Williams, M., Richardson, A. D., Reichstein, M., Stoy, P. C., Peylin, P., Verbeeck, H., ... Wang, Y.-P. (2009). Improving land surface models with FLUXNET data. *Biogeosciences*, *6*(7), 1341–1359. doi: 10.5194/bg-6-1341-2009
Wipfler, E. L., Metselaar, K., van Dam, J. C., Feddes, R. A., van Meijgaard, E., van Ulft, L. H., ... Bastiaanssen, W. G. M. (2011). Seasonal evaluation of the land surface scheme HTESSEL against remote sensing derived energy fluxes of the Transdanubian region in Hungary. *Hydrology and Earth System Sciences*, *15*(4), 1257–1271. doi: 10.5194/hess-15-1257-2011
Wulfmeyer, V., Turner, D. D., Baker, B., Banta, R., Behrendt, A., Bonin, T., ... Weckwerth, T. (2018). A new research approach for observing and characterizing Land–Atmosphere feedback. *Bulletin of the American Meteorological Society*, *99*(8), 1639 - 1667. doi: 10.1175/BAMS-D-17-0009.1
Xie, Z., Yuan, F., Duan, Q., Zheng, J., Liang, M., & Chen, F. (2007). Regional parameter estimation of the VIC land surface model: Methodology and application to river basins in China. *Journal of Hydrometeorology*, *8*(3), 447 - 468. doi: 10.1175/JHM568.1
Zhang, J., Wang, W.-C., & Leung, L. R. (2008). Contribution of Land-Atmosphere coupling to summer climate variability over the contiguous United States. *Journal of Geophysical Research: Atmospheres*, *113*(D22). doi: 10.1029/2008JD010136